Appendix B: Aerial Photograph Tables

All aerial photographs used in this study are cataloged in this appendix. Digital scans of these photographs are included with the DVD found at the end of this dissertation, in both raw TIFF and georeferenced GEOTIFF format.

Table B.1. Aerial photographs for sites included in the study.

Site		Aerial Photograph	Year
3BE245	Goforth-Saindon	AVP-4-77	1938
3BE245	Goforth-Saindon	AVP-5-11	1938
3BE245	Goforth-Saindon	AVP-1C-74	1941
3BE245	Goforth-Saindon	AVP-1C-83	1941
3BE245	Goforth-Saindon	AVP-1N-43	1943
3CN4	Point Remove	IA-4-26	1937
3CN4	Point Remove	IA-3B-8	1941
3CN4	Point Remove	IA-2N-6	1954
3FR1	Spinach Patch	AVU-8-77	1938
3LO15	Page	II-3C-201	1942
3LO15	Page	II-1N-16	1954
3LO208	Logan Eddy	II-1C-171	1941
3LO208	Logan Eddy	II-5N-11	1954
3MA22	Huntsville	F-15-97	1936
3MA22	Huntsville	F-82-8	1936
3MA22	Huntsville	CZO-2C-153	1942
3PP23	Scotia	IM-7-33	1937
3PP23	Scotia	IM-1N-14	1954
3PP49	Cove Creek	IM-3N-45	1954
3SB3	Cavanaugh	AWA-5-5	1938
3SB3	Cavanaugh	AWA-6-30	1938
3SB3	Cavanaugh	AWA-6-31	1938
3SB3	Cavanaugh	AWA-6-32	1938
3SB3	Cavanaugh	AWA-6-33	1938
3SB3	Cavanaugh	AWA-13-16	1938
3SB3	Cavanaugh	AWA-13-69	1938
3SB3	Cavanaugh	AWA-13-70	1938
3SB3	Cavanaugh	AWA-1N-11	1954
3SB3	Cavanaugh	AWA-1N-12	1954
3SB3	Cavanaugh	AWA-1N-13	1954
3SB3	Cavanaugh	AWA-1N-63	1954
3SB3	Cavanaugh	AWA01N-64	1954
3SB3	Cavanaugh	AWA-1N-65	1954
3WA1	Elkins	F-74-26	1936

Site		Aerial Photograph	Year
3WA1	Elkins	AWE-4C-77	1941
3WA1241	Goshen	F-16-13	1936
3YE15	Bluffton	AWF-12-85	1938
3YE15	Bluffton	AWF-1G-167	1950
3YE21	Berry	AWF-7-21	1938
3YE352	Carden Bottom Cem.	AWF-1-34	1938
3YE352	Carden Bottom Cem.	AWF-4G-71	1950
34AD11	Ewing Chapel Cem.	CFL-8-1	1940
34AD11	Ewing Chapel Cem.	CFL-2K-28	1952
34CK6	Harlan	BQH-6-52	1938
34CK6	Harlan	BQH-8K-86	1952
34CK43	Brackett	BQH-2-75	1938
34CK43	Brackett	BQH-12K-27	1952
34CK1/4	Reed	CFO-3-3	1939
34DL41	Lillie Creek	CFO-4-20	1939
34DL41	Lillie Creek	DFO-4-75	1939
34KF6	Victor Area	BQI-5-98	1938
34KF6	Victor Area	BQI-5K-36	1952
34LF9	Holson Creek	BQI-6-77	1938
34LF9	Holson Creek	BQI-6K-89	1952
34LF37/70	Spiro/Skidgel	BQI-3-57	1938
34LF37/70	Spiro/Skidgel	BQI-3-59	1938
34LF37/70	Spiro/Skidgel	BQI-3-65	1938
34LF37/70	Spiro/Skidgel	BQI-4K-96	1952
34LF37/70	Spiro/Skidgel	BQI-4K-172	1952
34LF117	Borrow Pit	BQI-4-15	1938
34MI45	Eufala	AWJ-1F-96	1949
34MS4/175	Hughes/Ft. Davis	CUE-8B-16	1941
34MS4/175	Hughes/Ft. Davis	CUE-7K-22	1952
34MS4/175	Hughes/Ft. Davis	CUE-7K-100	1952
34SQ12	Parris	BQM-2-40	1938
34SQ12	Parris	BQM-3K-88	1952
34WG2	Norman	AH-31-16	1936
34WG2	Norman	AH-31-17	1936
34WG2	Norman	AH-31-18	1936
34WG2	Norman	AWO-4-28	1938
34WG2	Norman	BQH-6-81	1938
34WG2	Norman	AWO-6-12	1940
34WG2	Norman	BQH-7K-136	1952

Table B.2. Aerial photographs for sites not included in the study (sites discussed at the end of Appendix A).

Site		**Aerial Photograph**	**Year**
3BO26	(Unnamed)	AVQ-1N-88	1954
3CN16	(Unnamed)	IA-2N-28	1954
3CN16	(Unnamed)	IA-2B-195	1941
3CN23	Morrilton Airport	IA-4-24	1937
3CN23	Morrilton Airport	IA-3B-11	1941
3CN23	Morrilton Airport	IA-2N-3	1954
3FR41	Holdar Bluff	AVU-3-89	1938
3FR115	Rock Ridge Farm	AVU-3-83	1938
3FR240	Fallen Indian House	AVU-7-78	1938
3FR240	Fallen Indian House	AVU-2N-140	1954
3LO11	(Unnamed)	II-3-10	1937
3LO27	Little Short Mountain Mounds	II-2C-24	1941
3SB2	Jake Ball	AWA-13-41	1938
3SB2	Jake Ball	AWA-13-40	1938
3SC22 & 3SC24 & 3SC29	Guy Grandstaff Place Oliver Airport E. A. Judy	CQU-4A-89	1940
3SE18	Gilley Farm	SBJ-3N-13	1954
3SE73	Landis	SBJ-2C-162	1942
3SE113	(Unnamed)	DBJ-2C-88	1942
3SE130	Wasson Hole	DBJ-2N-23	1954
3SE329	MaCmillan	DBJ-2C-123	1942
3WA820	King's Cemetery	AWE-5N-30	1954
34MS10	Mounts	CUE-9B-19	1941
34MS10	Mounts	CUE-8K-128	1952

Appendix C: GIS Procedures

All GIS procedures for this dissertation were performed with Idrisi Kilimanjaro v. 14.02. Idrisi default settings were used for all operations unless otherwise stated. Because of the size of the datasets (the base DEM is 13,338 columns by 10,112 rows, and the raster file is 526,851 kb), many of the procedures required significant processing time. Even simple overlay operations required 5 minutes or more when performed on the full-sized DEM, while more complex operations often required several hours of processing time. Most procedures were run on a personal laptop computer: Gateway 450e with Intel Pentium M processor 1.4 GHz, 768 MB DDR SDRAM, 40 GB hard drive. The procedures used for Monte Carlo viewshed analysis required more than 40 GB hard drive space (for each topographic region) and were therefore run on a Maxtor 250 GB external hard drive (2 MB cache buffer, USB 2.0 connection), with no significant loss of processing speed. Several procedures which returned insufficient memory errors on the personal computer were attempted on various desktop computers at the University of Arkansas' Center for Advanced Spatial Technologies (CAST) labs, with little noticeable increased performance or processing speed.

I believe that these minutiae of computing will seem quaint in fewer than ten years, in which time processing speed will far surpass any of the numerous technical limitations I encountered in this study. I only hope (rewording Greg Brown 1992:track 6) that my theoretical assumptions do not promise more than increased computing speed can endure.

Procedure for defining bottomlands

The procedure used for defining bottomlands within the study-area DEM (Chapter 7) is a novel approach and all steps involved are detailed here.

Key to procedure lists:

Idrisi module names given are in *italics*, GIS layers are given in ALL CAPS.
ORIGDEM = original digital elevation model, uncorrected for reservoirs.
DEM = base digital elevation model, corrected for reservoirs.

1) DEM *contract* 10 x in both directions to create DEM10x [to allow for pit removal processing with available computing resources].

2) *Pit Removal* on DEM10x to create PITFREE10x.

3) *Runoff* on PITFREE10x to create RUNOFF10x.

4) *Reclass* RUNOFF10x: 0 to 1000 = 0, above 1000 = 1 to create STREAMS10x.

5) *Buffer* 50 km from MAJORCENTERS (raster file copied from DEM where the location of major mound centers = 1, all else = 0); target and buffer zone = 1, non-buffer zone = 0 to create MAJORBUFFER.

6) Overlay MAJORBUFFER * STREAMS10x to create STREAMSB10x [eliminating streams more than 50 km from a major mound center].

7) *Rastervector* to convert (raster) STREAMSB10x to (vector) STREAMSB10x .

8) *Generalization* on (vector) STREAMSB10x through point selection, 5 km tolerance, to create STREAMPOINTS.

9) *Display* DEM with STREAMPOINTS, zoom in and scan all points, manually delete and re-digitize those that fall outside of bottomlands to the center of the nearest bottomland location.

10) *Rastervector* STREAMPOINTS from vector to raster, copying parameters from DEM (change cells to record the frequency of points) to create (raster) STREAMPOINTS.

11) *Overlay* STREAMPOINTS * DEM to create STREAMELEV [thus extracting DEM elevations at STREAMPOINTS locations].

12) *Rastervector* STREAMELEV to (vector points) STREAMELEV.

13) *TIN* on STREAMELEV (add corner points equal to the elevation of the point nearest each corner) to create TIN file STREAMTIN and DEM file STREAMDEM [any surface interpolation method could be employed here; TIN interpolation was chosen in this case because it was the only method which could be employed on the dataset given available computing resources].

14) *Map Calculator* DEM – STREAMDEM to create DEMDETRENDED [thus creating a DEM de-trended for stream gradients].

15) *Reclass* DEMDETRENDED: below 8 = 1, above 8 = 0 to create BOTTOMSPRELIM.

16) *Display* BOTTOMSPRELIM, manually digitize and overlay clearly recognizable bottomland areas which are not reflected in BOTTOMSPRELIM to create BOTTOMS.

Appendix D: Bottomland Proximity Tables

All bottomland proximity results from the four proximity methods discussed in Chapter 7 are presented here. This information is summarized by region in Figures 7.13-7.15 and Tables 7.2-7.5, by site echelon in Tables 7.6-7.9, and by site size within the Ozark region in tables 7.10-7.13

Table D.1. Straight-line distances, ha of bottomland within 10 proximity indices.

Distance index	1 (5 km)	2 (10 km)	3 (15 km)	4 (20 km)	5 (25 km)	6 (30 km)	7 (35 km)	8 (40 km)	9 (45 km)	10 (50 km)
Site										
3BE245	1830	3563	5318	9737	14925	20710	25985	32721	40877	52273
3CN4	5967	17859	34690	52957	73708	95170	111726	130890	151849	166966
3FR1	4385	11052	18272	28987	39169	54819	67342	82566	102285	125824
3LO15	3792	7158	9885	15815	24788	33303	50274	73071	101098	141977
3LO208	3378	7820	11490	15424	25207	41482	60478	82436	104083	137507
3MA22	1121	2159	4500	7297	9576	18169	27434	36215	42058	49578
3PP23	2472	9318	19304	28662	42899	61364	89295	113714	135815	159014
3PP49	3075	7923	17900	30415	45627	67477	87658	110975	137466	154704
3SB1	5078	15695	29391	39631	47622	64016	84643	104366	123379	145935
3S3	1136	10764	30310	44769	59622	83547	97616	116046	133677	160206
3SC1835	23	1118	8621	20102	30596	42942	58088	71686	89842	110496
3WA1	1667	5770	9415	11713	14224	20865	25559	35321	45000	52204
3WA1241	1403	4185	8763	14360	18796	30378	36061	39992	45604	51070
3YE15	4362	8614	14653	18655	31305	43570	53501	65271	75714	94250
3YE21	3815	6778	13588	19419	39742	55494	82463	113412	137103	155690
3YE352	5965	16281	29235	47567	73763	94157	113317	131593	155939	178422
23MD46	953	3690	6250	8637	12777	16203	19925	29118	43634	59233
23SN42	3847	10370	16657	22222	27000	31417	39718	46007	52200	60156
34AD11	774	1224	2917	5168	9345	14310	23095	34622	52621	74894
34CK6	2577	6576	13990	27419	37187	54722	74520	99841	121889	145657
34CK43	1547	4187	7607	10529	17848	25526	38026	53280	75539	108324
34DL1	1564	4473	11590	17394	23320	35537	48239	67464	84332	100887
34DL41	1460	3470	8385	17681	30472	42410	54482	67747	86720	104627
34LF6	4490	11567	17883	28005	43308	55020	64844	81551	102507	123456
34LF9	4300	10672	17395	26107	36317	50069	62858	77028	90313	108008
34LF16	3809	8687	14813	20424	29629	45139	57838	71774	90187	109353
34LF37	5732	18273	32404	41745	59319	77474	99616	123507	141988	161069
34LF70	4953	17610	32453	41965	57950	77504	99822	122631	141356	161623
34LF117	2765	7446	12690	23545	33638	40879	50352	66605	77437	86245
34MI45	1587	8475	13661	22727	33108	54602	77201	103506	126198	160345
34MS4/175	4212	13574	21904	32501	46320	66161	88216	108224	125223	150159
34MS52	1684	11987	23800	34602	49203	64233	85739	105457	128561	156191
34SQ12	1684	3270	5160	13107	26937	44726	69860	95240	120924	141164
34WG2	1854	6236	16845	29886	43662	57384	78247	102884	127688	147634

Table D.2. Simple cost model, ha of bottomland within 10 proximity indices.

Distance index	1	2	3	4	5	6	7	8	9	10
Site										
3BE245	1838	2808	3045	3131	3465	4408	5426	7308	9662	12392
3CN4	24746	49397	65313	75877	114716	138046	147179	156470	171001	178325
3FR1	24746	42917	55307	63418	73869	79826	87764	95359	97588	100627
3LO15	2069	3194	4510	5625	6332	7062	7813	8893	11333	16178
3LO208	3585	4641	6978	8359	9198	10861	14653	17863	20772	22476
3MA22	7338	13036	1675.01	21882	23601	24529	2554.02	2609	26435	27175
3PP23	33580	65751	91512	109830	119190	131852	139225	141940	146217	149230
3PP49	24723	49020	85347	108682	134038	159823	173835	182653	188378	192671
3SB1	7558	32233	48744	55281	59421	64551	69022	75876	87534	96403
3S3	22	12661	34406	43860	51392	59598	72585	82017	97371	103729
3SC1835	0	0	0	0	0	0	0	0	2.091	4602
3WA1	4455	5245	6428	7555	8841	10262	12037	13342	14798	17240
3WA1241	234	996	4622	7391	8438	9221	10720	12517	14310	16372
3YE15	4398	8018	10286	11723	12464	13087	13980	14333	14721	15249
3YE21	7777	12379	17630	23698	26431	29765	32652	38082	41079	46031
3YE352	40535	81041	95888	116379	140069	154484	167096	178344	182586	186040
23MD46	7423	12065	15114	17483	20959	26936	33211	46365	58497	74491
23SN42	3758	4278	7280	9351	13828	14776	15953	16359	17127	17683
34AD11	6216	9339	11619	16848	20978	2667.03	35908	4131	48094	55618
34CK6	2410	13657	38177	65877	82894	110496	130941	144139	155175	164361
34CK43	3276	4308	4635	5139	7507	8494	11444	13925	16374	30807
34DL1	1537	2634	4134	8675	21279	38378	44611	54081	62209	67185
34DL41	1113	1683	1829	4319	12550	28834	47459	62459	72190	84792
34LF6	8450	15676	19510	22520	30531	37396	42558	47640	51888	65639
34LF9	7291	12478	15273	19297	22278	25060	27052	30058	33794	37236
34LF16	3892	7453	13862	20501	23916	27881	30473	34361	36827	39677
34LF37	17750	43136	54685	73513	99293	117195	134023	142144	149388	158557
34LF70	9448	40730	60432	88135	100895	117562	134625	143655	151521	161096
34LF117	1155	3219	9680	15354	19516	29749	36687	41475	45612	49734
34MI45	3723	10384	15471	20676	62045	102480	130490	146418	164523	177177
34MS52	41452	75888	107837	144157	170852	191660	200845	217478	232055	241333
34MS4/175	13237	52448	82973	117376	139010	151992	167411	179429	186750	198750
34SQ12	984	1792	2353	2742	3164	3557	4003	22012	44661	61133
34WG2	2025	10898	37126	65717	86104	110690	134475	147791	158760	167180

Table D.3. Rivers as barriers model, ha of bottomland within 10 proximity indices.

Distance index	1	2	3	4	5	6	7	8	9	10
Site										
3BE245	2277	250	2798	5116	6146	9345	12763	16017	19068	22812
3CN4	845	11934	15529	19200	31426	47669	49467	50028	51031	51354
3FR1	16834	21138	21559	2168	21712	21856	21892	22253	22942	23014
3LO15	8048	1388.01	20619	25635	29702	31354	32803	35171	41393	45239
3LO208	7391	13653	15289	17874	22156	25335	30288	35235	4060	52326
3MA22	2607	6437	7577	8322	9256	10212	11443	11653	11792	1198
3PP23	4551	51107	53434	5377	54265	5447	5506	55071	55145	5620
3PP49	1554	11008	14231	14728	15081	16721	17352	21189	22448	22957
3SB1	1595	2746	3168	4138	4348	6322	7002	9026	10212	11072
3S3	21	2087	6035	7840	8606	9008	10192	11603	12202	12535
3SC1835	0	0	0	0	0	0	0	0	2.091	23281
3WA1	22459	24462	2528.04	25523	25792	2631.08	26744	27051	2716.03	27567
3WA1241	641	143	308	5116	7139	9986	10665	11299	12949	13427
3YE15	14118	39679	5125.09	55671	61539	64889	67649	69396	69829	69998
3YE21	3663	5255	6286	7361	8241	8643	8723	8827	9365	10348
3YE352	6510	11014	11926	11961	11968	12077	12958	14225	15446	17730
23MD46	17193	23264	23942	269.06	37895	42759	44894	547.048	61876	63742
23SN42	673	8371	10878	11325	16707	17515	2164	23842	2418	26784
34AD11	1404	3578	513	802.03	8742	9952	12405	1586.05	19962	22681
34CK6	5706	15708	19705	21666	24508	26339	26731	27316	27627	27913
34CK43	666.01	8732	9001	9759	11024	11339	13634	14186	15353	15579
34DL1	226.03	3857	12795	1807.01	25204	2652	26938	31305	32745	35372
34DL41	255	344	473	2272	7022	13891	15950	20083	27625	33536
34LF6	8584	14725	2044	26318	36211	40347	44196	52389	59259	66304
34LF9	10333	2169.05	33356	35428	3848	39533	40275	4143	42485	42555
34LF16	14273	22415	30301	35516	40213	42121	42796	44346	45653	4785.02
34LF37	8382	8993	9647	10268	10609	11311	17391	17491	19571	20106
34LF70	4456	8998	9880	10173	10868	17136	17482	17661	20078	20397
34LF117	1939	5071	25883	4698	64531	70224	70865	72147	72953	73277
34MI45	1005	1204	3419	5099	7361	9211	12954	15329	19110	23294
34MS52	16832	20619	2277	24258	24783	3144	31941	32423	33812	34924
34MS4/175	537	3200	4291	4841	9718	17736	20587	21677	23236	24808
34SQ12	4953	7402	7469	7729	8074	8381	9684	10316	12424	1298
34WG2	532	1100	5001	11024	16118	19285	22121	28826	31588	32643

Table D.4. Rivers as corridors, ha of bottomland within 10 proximity indices.

Distance index	1	2	3	4	5	6	7	8	9	10
Site										
3BE245	1681	2755	3439	4241	5275	11375	12196	15102	17194	20726
3CN4	16040	34536	50052	65097	78642	88447	106564	126042	142486	159562
3FR1	4782	8761	22473	28721	36257	42875	48627	54349	65381	76773
3LO15	3954	5741	7311	9307	11502	14396	17589	20245	31652	44170
3LO208	5731	7244	8247	9252	11560	14794	26081	37591	45966	50099
3MA22	2292	3689	4281	4572	6987	11103	18068	20593	29242	32213
3PP23	15486	32000	47908	67992	82718	91092	110743	131034	147507	156168
3PP49	17379	32211	46241	60754	75884	86859	102369	122875	138707	154339
3SB1	1566	10712	19879	29361	39068	47394	54680	61536	70940	80842
3S3	17	1407	9913	22434	35236	45151	53524	63476	83649	95332
3SC1835	0	0	290	583	1133	4428	8090	13108	17361	23760
3WA1	5923	8238	9670	11887	13543	14633	16134	20003	28389	34536
3WA1241	8521	9616	11282	12747	14462	17907	19578	23087	26959	35321
3YE15	4448	6743	8490	9830	12294	14233	16187	17660	18573	20477
3YE21	5919	11103	14370	16729	21855	37571	47618	53547	58412	66658
3YE352	2243	19416	37943	54175	68314	82777	104003	125994	144589	158342
23MD46	2633	2995	3958	6232	8372	11766	17562	22146	26291	32872
23SN42	4814	9799	14238	19923	21779	24434	27278	31217	34450	37725
34AD11	2646	4408	4886	5135	5536	8388	14320	26380	35802	43796
34CK6	4824	12613	27749	52035	75622	99992	114539	123517	138984	147075
34CK43	4090	5392	8749	10402	11808	14886	16921	20183	29868	40166
34DL1	2102	4763	9038	14652	33968	41873	44961	49476	55940	65510
34DL41	1624	1920	4730	6554	10604	22671	32537	40466	46281	65020
34LF6	6703	14328	18969	22468	25519	29333	34753	46094	55019	59731
34LF9	5028	9935	15021	20292	23822	27140	33457	37986	40918	45380
34LF16	3021	5586	7579	11580	16672	21250	27441	33253	38204	42237
34LF37	6103	14944	26195	42640	57904	74581	87718	100959	111342	130073
34LF70	3036	10655	25894	36179	53764	72224	90087	102710	120466	132207
34LF117	2958	8411	14281	19487	23608	26836	33406	43447	48390	54642
34MI45	1885	3703	10665	25179	28918	36451	45711	59440	69493	84963
34MS52	23307	43344	62670	84568	104681	119397	131072	149837	176975	195873
34MS4/175	5252	18903	43592	75139	98397	113911	130945	150838	159536	166222
34SQ12	2408	9329	18488	28170	37103	52008	65371	73699	87526	103610
34WG2	3690	8940	18495	43289	65218	91255	111736	119726	134096	145497

Appendix E: Nearest-Neighbor Analysis and Proximity Models

Distances between sites are sometimes used in the estimation of territorial size. Recently, for example, Blitz (1999) concludes that distances between mound centers in the South Appalachian area are better explained by the sociopolitical fission-fusion process, rather than simple vs. complex chiefdoms. Peebles (1978) employed 1st, 2nd, and 3rd-nearest neighbor distances in a study of Mississippian settlements in the Moundville area. In perhaps the most elaborate of such studies, Hally (1993, 1996, 1999) differentiates between simple and complex chiefdoms by measuring the straight-line distances between mound construction episodes or site components at contemporaneous mound centers. Applied to Mississippian civic ceremonial sites in northern Georgia (sites with at least one platform mound), Hally concludes that (with exceptions) contemporaneous centers less than 18 km from one another constitute elements of the same complex chiefdom, while any center more than 32 km from another contemporaneous center constitute an independent, simple chiefdom (1993:159; 1996:98, 1999:104). These conclusions are based on a bimodal distribution of nearest-neighbor distances between contemporaneous sites, with relatively few sites occurring between 18 and 32 km (Figure E.1).

Hally uses straight-line distances as a proxy for travel time/ease of communication between sites because contemporaneous centers in northern Georgia are generally located along different rivers, and the importance of river travel in the area has not been documented, while overland trails have been (Hally 1993:148).

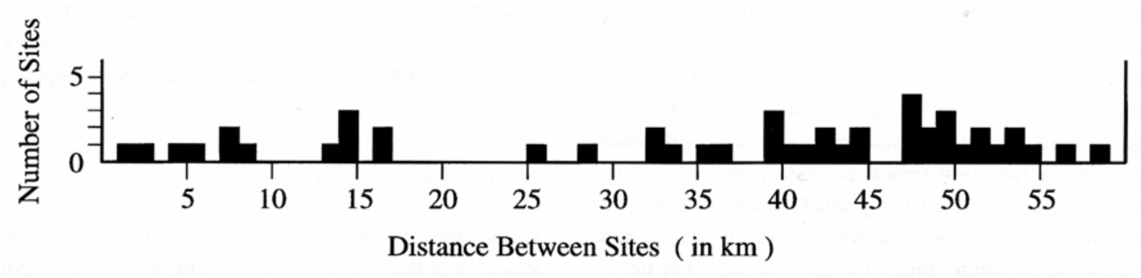

Figure E.1. Hally's plot of the spacing of contemporaneous construction episodes in Mississippian mound sites in northern Georgia (1999:103). Few sites occur between a distance of 18 to 32 km.

The analysis presented here is not intended to replicate exactly the methodology used in nearest-neighbor distance analyses. The current study area contains fewer civic ceremonial centers than those in northern Georgia (only 22 are used here), and any conclusions would therefore be less robust. Even more problematic is the question of timing. The chronological framework for sites in the current study area is very poor, and without an understanding of which sites are contemporaneous, archaeological conclusions from nearest-neighbor analyses would be spurious. This analysis is only intended to test the divergence of results of nearest-neighbor analysis using four different proximity models.

Distances between sites in the Arkansas Basin and adjoining regions were calculated using the four different proximity models discussed in Chapter 7. For each site, a distance surface was calculated as straight-line distances, and with the simple cost, river barrier, and river corridor models. From each of these surfaces, the location of all other sites was used as a masking layer to extract distance values. Because the method is not subject to edge effects (as long as all sites are within the GIS layer used to generate the surfaces), sites in the Ouachita and Arkansas River 2 Region are included. Following

Hally, only sites with platform mounds are used. Loftin is in a reservoir uncorrected for topography and is omitted here.

Using GIS, not only nearest neighbor distances, but second-nearest neighbor, third-nearest neighbor, and so on, can be calculated quite easily. Figure E.2 shows straight-line distances calculated for all major centers within the study area. While the interpretive potential of the high-order nearest neighbors is doubtful (the 21st nearest neighbor simply shows how far the farthest center is from each center), trade between sites of far greater than 250 km distance is clearly established (between Spiro and Cahokia, for example), and the patterns of site clustering at this scale may have significance when compared to those of completely different regions.

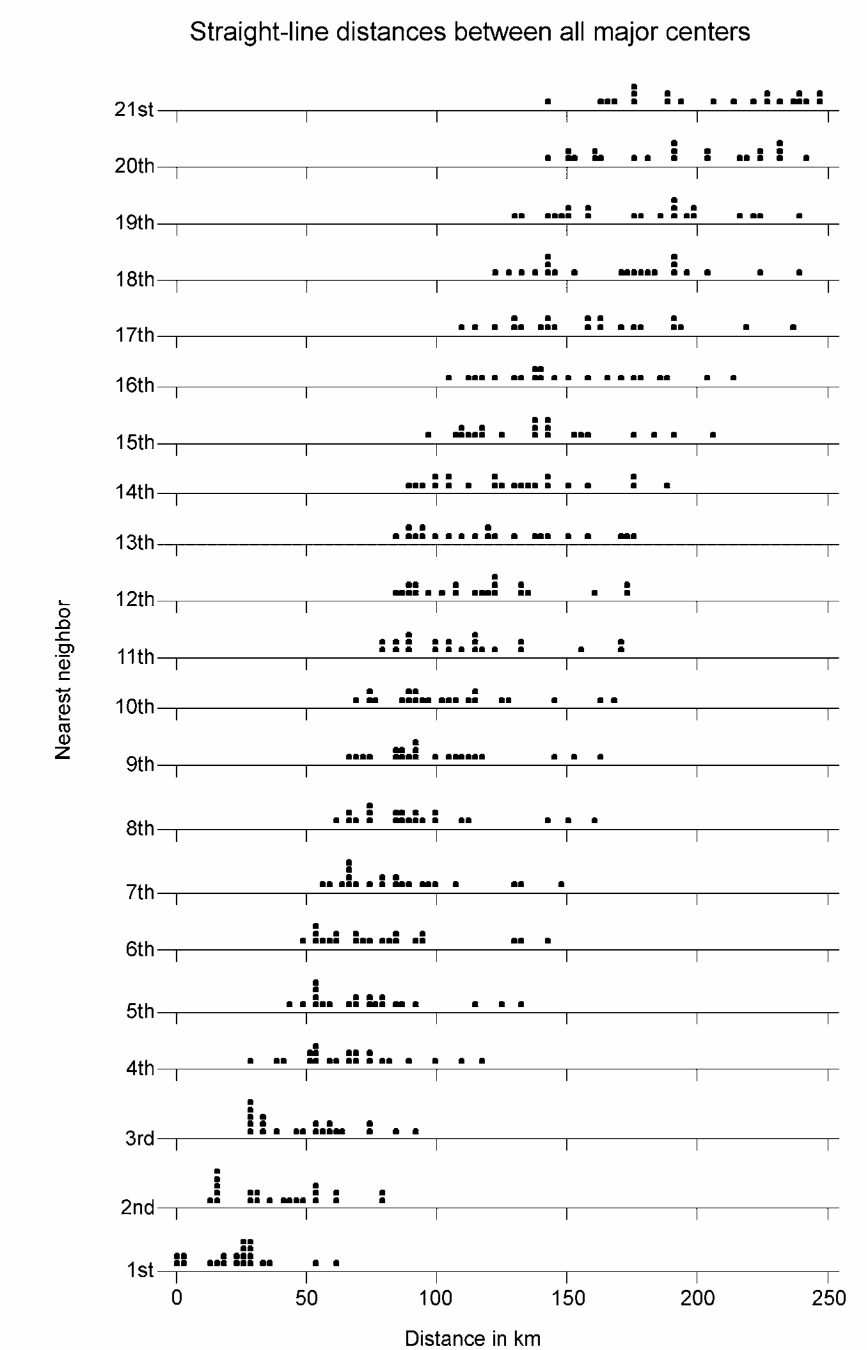

Figure E.2. Straight-line distances between all 22 major centers, showing 1st nearest neighbor, 2nd nearest neighbor, etc. up to the farthest neighbor (21st) from each site.

Note the shifting clusters of sites at each successive step in the graph. Four sites form a very tight group very short distances from one another on the 1st nearest neighbor plot: Spiro, Skidgel, Norman, and Harlan. These sites are all at least roughly contemporaneous with one another, and Spiro, Norman, and Harlan are the largest ceremonial centers in the study area. Spiro and Skidgel are likely related, but are treated as two sites here.

Figure E.3 shows the 1st and 2nd nearest neighbor for all major centers within the study area, calculated with the four different models. Recall that only the straight-line distance model has an empirical scale (km). The other three models are expressed in arbitrary friction units, 'calibrated' to the straight-line scale as discussed in Chapter 7. For this figure, each plot has been scaled to express a full range of measurements from the nearest 1st nearest neighbor to the farthest 2nd nearest neighbor. In this way, the scales are at least roughly comparable; each expresses the full range of values scaled to one another.

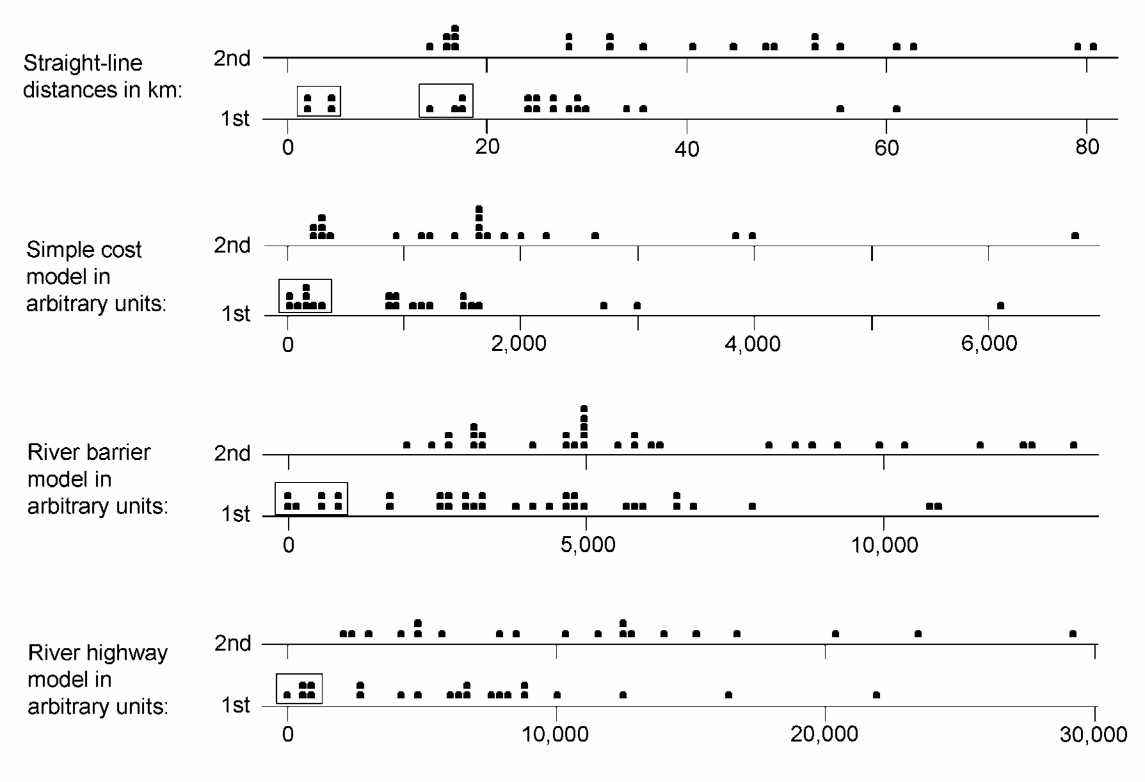

Figure E.3. 1st and 2nd nearest neighbors for all major centers, calculated with four different distance models. Note that the scale for each model is different. For this figure, each plot has been scaled to encompass the nearest 1st nearest neighbor, and the farthest 2nd nearest neighbor. Boxes outline site clusters shown in Table E.10.

Disregarding the question of whether or not the sites are contemporaneous, there are several clusters within the data that offer clues to the compatibility of the different models. Table E.1 shows the 1st nearest-neighbor sites from Figure E.3, tracing the migrating rankings of some of the sites from one model to the next. In the straight-line model there are two clusters between 0 and 20 km. In the simple cost model the same sites unite into one cluster. Taking rivers into account, either as barriers to travel or corridors of travel, moves some of these sites out of the lowest cluster and others in. At the lower end of the rankings sites are equally mobile, moving from one cluster to another between the proximity models.

The only centers consistently nearer other centers in all four models are Skidgel and Spiro (which may more appropriately be considered a single site), and Norman and Harlan. The only centers consistently farthest from others (in Hally's analysis, those most likely to be independent centers) are Loftin, Borrow Pit, and Bluffton in three of the four proximity models.

While the question of timing does not allow this analysis to add much to the archaeological interpretation of this region at present, the methodological caution is clear: straight-line distances return a different picture of patterning than do friction models, and friction models with different theoretical assumptions (whether rivers are barriers or corridors to movement, or do not matter) return results even more divergent.

Table E.1. Ordinal ranking of sites by nearest-neighbor distances. Boxes outline site clusters as shown in Figure E.19.

Straight line distances	**Simple cost model**	**Rivers as barriers**	**Rivers as Highways**
1st neighbor	**1st neighbor**	**1st neighbor**	**1st neighbor**
Spiro	Spiro	Spiro	Harlan
Skidgel	Skidgel	Skidgel	Norman
Norman	Crd Btm Cem	Cavanaugh	Spiro
Harlan	Harlan	Page	Skidgel
Cavanaugh	Norman	Pineville	Point Remove
Hughes/Ft. D	Point Remove	Reed	Crd Btm Cem
Point Remove	Cavanaugh	Norman	Hughes/Ft. D
Crd Btm Cem	Hughes/Ft. D	Harlan	Parris
Reed	Reed	Gfth-Saindon	Cavanaugh
Lillie Creek	Parris	Point Remove	Brackett
Page	Brackett	Hughes/Ft. D	Ew Chp Cem
Logan Eddy	Lillie Creek	Lillie Creek	Logan Eddy
Ew Chp Cem	Borrow Pit	Crd Btm Cem	Reed
Parris	Gfth-Saindon	Ew Chp Cem	Gfth-Saindon
Bluffton	Ew Chp Cem	Parris	Page
Huntsville	Logan Eddy	Logan Eddy	Lillie Creek
Elkins	Page	Brackett	Huntsville
Brackett	Pineville	Elkins	Elkins
Gfth-Saindon	Elkins	Huntsville	Pineville
Pineville	Huntsville	Bluffton	Bluffton
Borrow Pit	Bluffton	Borrow Pit	Loftin
Loftin	Loftin	Loftin	Borrow Pit

Appendix F: Contents of DVD Included with this Dissertation

File	Contents
Readme.txt	Brief explanation of contents of DVD.
Vgl_dis.pdf	This dissertation in PDF format (split into sections).
AERTIFF	Folder containing scans of all aerial photographs used in this dissertation in raw TIFF format. Also contains text file with brief explanation of the scanned aerial photographs.
AERGEO	Folder containing scans of all aerial photographs used in this dissertation in georeferenced GEOTIFF format. Also contains text file with brief explanation of the georeferenced aerial photographs and metadata.
DEMRES	Folder containing DEMs of four reservoirs corrected for pre-reservoir topography:

GLOC	Grand Lake O' the Cherokees
FTGIBS	Fort Gibson Lake
RSKERR	Robert S. Kerr Lake
EUFALA	Eufala Lake

Also contains text file with brief explanation of the corrected reservoirs and metadata.